Bull. Mater. Sci., Vol. 35, No. 4, August 2012, pp. 617–621. © Indian Academy of Sciences.

Solid state synthesis and photoluminescence of $Sr_3Y(P_xV_{1-x}O_4)_3$: Eu^{3+} submicrocrystalline rod

XIUZHEN XIAO and BING YAN*
Department of Chemistry, Tongji University, Shanghai 200092, China

MS received 9 October 2010; revised 18 January 2011

Abstract. **Using rare earth coordination polymers with ortho-hydroxylbenzoic acids as rare earth species and composing with organic polymers as the hybrid precursors, $Sr_3Y(P_xV_{1-x}O_4)_3$: Eu^{3+} (x = 0·1, 0·3, 0·5, 0·7, 0·9) phosphors has been synthesized. These phosphors present the column-like particles with a width of 250 nm and a length of 1 μm. The value of red emission to orange emission for Eu^{3+} varies with the V content, indicating that the RO (red/orange) value increases with the increase of V content due to the lower electronegativity of V. $Sr_3Y(P_{0.3}V_{0.7}O_4)_3$ has been shown to be the best composition among different compositions. Furthermore, the concentration quenching of Eu^{3+} in $Sr_3Y(P_{0.3}V_{0.7}O_4)_3$ took place and the optimum concentration of Eu^{3+} is 5 mol % in the range of 1–9 mol %.**

Keywords. **Phosphors; chemical synthesis; luminescence.**

1. Introduction

Rare earth ions are well known luminescent activators in a variety of host lattices and the rare-earth activated phosphors have been studied extensively because of their high light output, excellent colour rendering index, energy efficiency and greater radiation stability (Blasse and Grabmeter 1994; Burland *et al* 1994). Eulytite phosphates have been shown to be better hosts for rare earth ions (Kaminskii *et al* 1976; Rogemond *et al* 1985). The photoluminescent behaviours under VUV–UV excitation of $M_3La(PO_4)_3$: Ce^{3+} (M = Sr, Ba) phosphors and Ce^{3+}, Pr^{3+}, Tb^{3+} activated $Sr_3Ln(PO_4)_3$ ones have been reported detail (Hoogendop *et al* 1994; Liang *et al* 2004). The syntheses of conventional rare earth phosphors mainly focus on the high-temperature solid-state reactions, which can permit to easily change the structural characteristics of the powders (Yan *et al* 2006). Recently, the development of new methods for the preparation of micron or submicron or nano phosphors may increase the possibilities for high effective rare earth phosphors (Dhanaraj *et al* 2001; Nair *et al* 2000; Kang *et al* 2003). For example, the sol–gel technology based on hydrolysis and polycondensation process is the most popular, which has been verified to be very useful in the synthesis of non-agglomerated nanoparticles with surface accessibility for treatment (Okamoto and Yamamoto 2001). Additionally, the hydrothermal process is also employed widely in the synthesis of rare earth ion-doped inorganic compounds (Stouwdam and Van Veggel 2002; Huignard *et al* 2003). Recently, we put forward a new method to phosphors which are produced by thermal treatment of hybrid materials (Xiao and Yan 2006; Huang and Yan 2007). In this method, rare earth complex of aromatic carboxylic acid (ortho hydroxylbenzoic acid) is used as the rare earth species. The advantages of the aromatic carboxylic acid are to coordinate rare earth ions to form corresponding rare earth coordination polymers with infinite chain structure (Chuai *et al* 2000). Then rare earth coordination polymers can be combined with organic polymers, polyacrylamide (PAM), polyethylene or polyvingyl alcohol (PEG or PVA) as dispersing medium template and urea as a fuel to form the interpenetrating polymers network structures for their similar polymeric chain structures. During the procedure of preparation of rare earth luminescent materials, the morphology and particle size can be controlled when rare earth oxides are *in situ* achieved from the hybrid precursors.

In this context, we have fabricated $Sr_3Y(P_xV_{1-x}O_4)_3$: Eu^{3+} luminescent materials with different vanadium contents. Rare earth coordination polymers with ortho-hydroxylbenzoic acids are used as rare earth species and composed with organic polymers as the hybrid precursors, which can be used to produce slighter agglomerated and well-dispersing materials (Huang and Yan 2004; Yan and Xiao 2006). This pathway exhibits different advantages, mainly the implementation of soft temperatures to produce the materials. Accordingly, a control on the structure, morphology of particles, dispersion of different metals, etc is also possible. Furthermore, we have investigated the influence of vanadium content on the luminescence of Eu^{3+} to find the optimum composition. Then we have discussed the effect of europium concentration on the luminescent properties of Eu in detail.

*Author for correspondence (byan@tongji.edu.cn)

2. Experimental

2.1 *Synthesis of $Sr_3Y(P_xV_{1-x}O_4)_3$: Eu^{3+}*

The initial material, Y_2O_3, was firstly dissolved into concentrated nitric acids. Then superfluous salicylic acid (6·0 mmol) was dissolved into 95% ethanol and its pH value was then adjusted to 7 ∼ 8 with ammonia solution. Then the 1 mmol $Y(NO_3)_3$ and 0·05 mmol $Eu(NO_3)_3$ was added and mixed homogenously. After stirring for 1 h, the urea and PEG were added into the above solutions with appropriate ratio to RE. After an hour, the solutions were heated to 70°C and the pH value was adjusted to 7 ∼ 8. At the same time, the $NH_4H_2PO_4$, $SrCO_3$ and NH_4VO_3 powders were added into the solution. After this, the solutions are stirred until they became homogenous systems. After being deposited for several days, they were filtered and the precursors were achieved. Finally the samples were heat-treated at 1100°C for about 5 h.

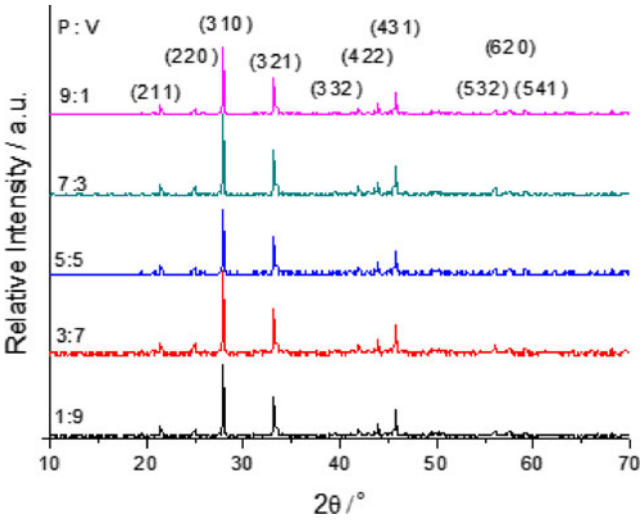

Figure 1. Selected XRD pattern of $Sr_3Y(P_xV_{1-x}O_4)_3$: 5%Eu^{3+} from hybrid precursors.

2.2 *Physical measurements*

The particle sizes were characterized by means of X-ray diffraction (XRD, Bruke, D8-Advance, 40 kV and 20 mA, CuKα). The morphology and microstructure were characterized by scanning electronic microscope (SEM, Philps XL-30). Excitation and emission spectra at room temperature were determined using Perkin-Elmer LS-55 model fluorophotometer (excitation slit width, 10 nm, emission width, 5 nm).

3. Results and discussion

XRD patterns of prepared samples are measured by X-ray powder diffraction using CuKα radiation. They have similar features except for the diffraction peak intensity. The representative one of $Sr_3Y(P_xV_{1-x}O_4)_3$: Eu^{3+} powders is shown in figure 1. All the diffraction lines in XRD pattern indicate that $Sr_3Y(P_xV_{1-x}O_4)_3$: 5% Eu^{3+} powders are single cubic phases and belong to the large family of the eulytite type compounds (Szuszkiewicz and Znamierowska 1990), which is in good agreement with those in JCPDS cards 44–0320. Besides this, phosphates and vanadates share the common physical and chemical properties, hence, we can inter-exchange these ones. Herein, the presence of vanadium cannot constitute an obstacle to make single phase solid solutions.

We further used the scanning electron microscope (SEM) to measure the $Sr_3Y(P_{0.3}V_{0.7}O_4)_3$: 5% Eu^{3+} samples. Figure 2 shows the representative SEM micrograph for $Sr_3Y(P_{0.3}V_{0.7}O_4)_3$: 5%$Eu^{3+}$. It can be seen that the product presents column-like morphology with a width of 250 nm and length of about 1 μm. Because of the high temperature (1100°C) of thermal decomposition, some conglomeration also can be observed in the morphology. It has been observed that crystalline powder and micrometer dimension for these powders with high strength would be very useful for the application to obtain high efficient phosphors because these microcrystalline materials can result in the high luminescent intensities (Pizani *et al* 2000). Until now, there have been a few reports about the synthesis of $Sr_3Y(P_{0.3}V_{0.7}O_4)_3$: 5%$Eu^{3+}$ with well morphology and dispersion at high temperature (1100°C) of thermal decomposition. In order to explain such morphology, we guess that rare earth complexes with aromatic carboxylic acid (ortho hydroxylbenzoic acid) show polymeric structure (Chuai *et al* 2000) and are used as precursors to prepare the luminescent species. The organic polymer, polyethylene glycol (PEG), is combined both as dispersing medium and fuel to form the

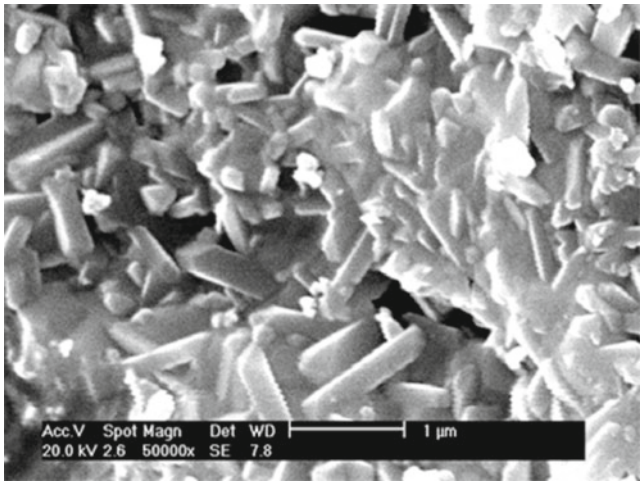

Figure 2. SEM of $Sr_3Y(P_{0.3}V_{0.7}O_4)_3$: 5%$Eu^{3+}$ from hybrid precursors.

polymeric hybrid precursor template and showed higher temperature of thermolysis process. These rare earth coordination polymers can combine with organic polymers (PEG) to obtain an interpenetrating polymeric network structures as they show similar infinite polymeric structure. Using the hybrid polymer as the precursors, it is possible that the particle sizes of rare earth oxysalts can be controlled and determined. Up to now, there have been a number of reports on the methods used based on the decomposition of precursors containing an organic additive like EDTA and its derivatives, citrate gels, acetate, oxoacetate, loctate, or oxalates which are successfully implemented (Rullens *et al* 2006; Alifanti *et al* 2003). These organic polymers are able to interact with metal ions. Sometimes, the organic polymers employed can serve both as a fuel for the nanocrystal formation and as a dispersing medium, limiting the agglomeration of particles (Zhou and Yan 2006). Therefore, this preparation technology connects the assembly of hybrid material with synthesis of micrometer material, which can be expected to be a candidate for the synthesis of other luminescent materials based on rare earth oxides.

The excitation spectra of 5%Eu^{3+}-doped $Sr_3Y(P_xV_{1-x}O_4)_3$ phosphors (x = 0·1, 0·3, 0·5, 0·7, 0·9) are depicted in figure 3(a), showing that the effective energy absorption mainly took place in the narrow ultraviolet region of 200–300 nm. The excitation spectra of all Eu^{3+}: phosphors, which are taken at an emission wavelength of 613 nm, consist of three bands centred at 223, 243 and 256 nm, respectively. The peak at 256 nm is ascribed to the charge transfer state resulting from the ligand O^2–2p orbit to the empty states of 4f configuration (Eu–O) transition. From the excitation spectra, we can find that the peak position of charge transfer band (CTB) for O^{2-}–Eu^{3+} in $Sr_3Y(P_xV_{1-x}O_4)_3$ shifts to longer wavelength with the increase of V content. According to the literature, the peak position of CTB (O^{2-}–Eu^{3+}) is strongly relative to the degree of covalency of Eu^{3+}-ligand bond (Su *et al* 1989). When we consider the bond structure of Eu^{3+}–O^{2-}–P^{5+} (V^{5+}), the above result can be explained. The P has a larger electronegativity and attracts electrons of O^{2-} more strongly, so that the electron cloud density of the O^{2-} ion decreases and it needs more energy for the electron transfer from O^{2-} to Eu^{3+}. As a result, the peak position of CTB shifts to longer wavelength with the increasing of V content. Additionally, the peaks at 220 and 243 nm are ascribed to the host band originating from the VO_4^{3-} group and PO_4^{3-}, indicating the existence of the efficient energy transfer from the host band to the activator.

Under the excitation in CTB (O^{2-}–Eu^{3+}) band, the emission spectra of 5%Eu^{3+}-doped $Sr_3Y(P_xV_{1-x}O_4)_3$ phosphors (x = 0·1, 0·3, 0·5, 0·7, 0·9) consist of the characteristic lines from low energy level $^5D_0$ to ^7F_J (J = 0, 1, 2, 4) of Eu^{3+}. Of these, the $^5D_0$–$^7F_2$ transition has been found to be the strongest in intensity compared to other transitions, which shows the Eu^{3+} in $Sr_3Y(P_xV_{1-x}O_4)_3$ host lattices is located at a low symmetry local site. While the Eu^{3+} site lacking inversion centre is favourable for the electric dipole transition as a forced transition ($^5D_0$–$^7F_2$) due to the admixture of the odd parity states, the Eu^{3+} site with inversion centre is favourable for the magnetic dipole transition ($^5D_0$–$^7F_1$). Furthermore, it is worthy to point out that we can also

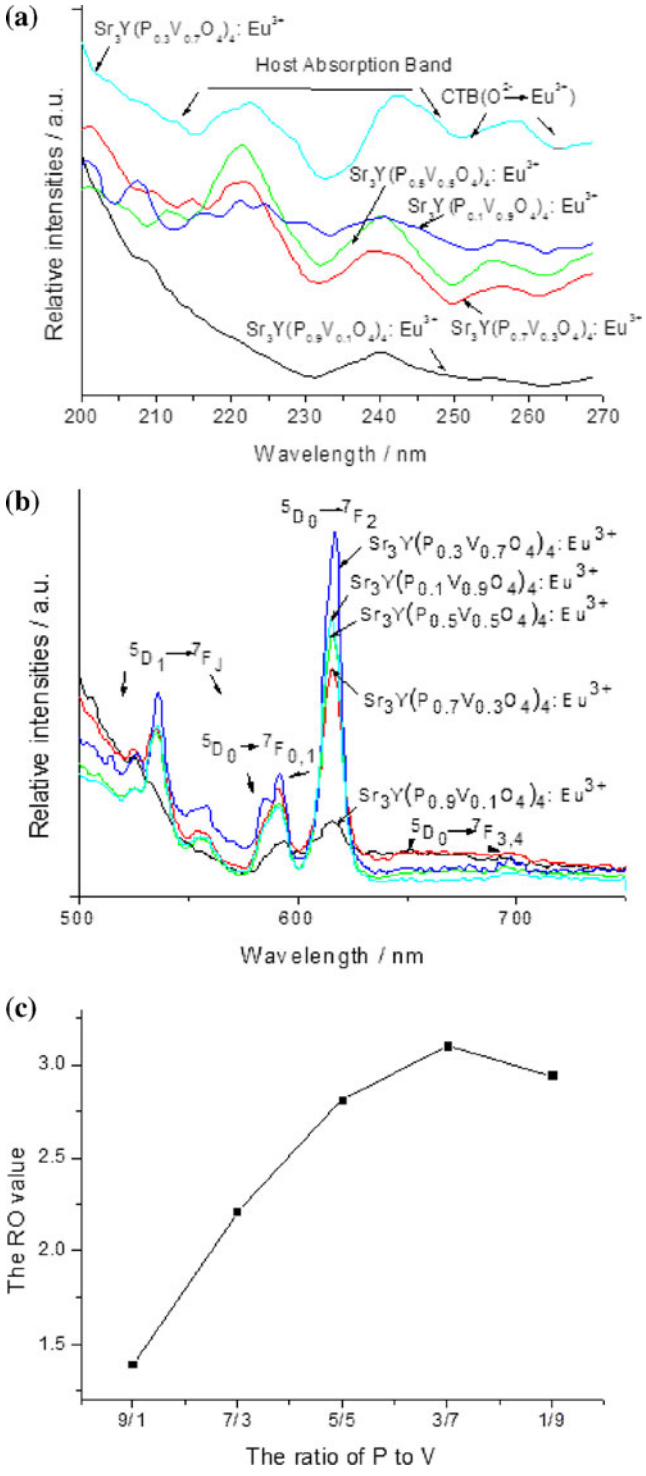

Figure 3. Excitation (A) and emission spectra (B) of $Sr_3Y(P_xV_{1-x}O_4)_3$: 5%Eu^{3+} with different content ratios of P to V (x = 0·1, 0·3, 0·5, 0·7, 0·9); change of ratio values of red to orange emission intensities (RO values) with content ratio of P to V (C).

observe weak emission corresponding to the $^5D_1 \rightarrow {}^7F_J$ ($J = 1, 2, 3, 4$) transition of Eu^{3+} from its high excited state of $^5D_1$ level in both emission spectra. The presence of emission from the higher energy is attributed to the low energy vibration of $(P_xV_{1-x})\ O_4^{3-}$ groups. The multiphonon relaxation by these complexes is not able to bridge the gaps between higher energy levels, resulting in weak emissions from these higher levels (Yu *et al* 2002). We also investigated the dependence of $^5D_0 \rightarrow {}^7F_2$ emission intensity for Eu^{3+} on the content of PO_4^{3-} or VO_4^{3-}. From figure 3, it also can be observed that the luminescent intensity reaches the strongest in $Sr_3Y(P_{0.3}V_{0.7}O_4)_3$: Eu^{3+} (A) although different compositions has little influence on the luminescent intensity. Besides this, we have investigated the influence of the matrix composition on the ratio value of red to orange for Eu^{3+}. It is well known that the Eu^{3+} $^5D_0 \rightarrow {}^7F_2$ transition is hypersensitive electronic dipole transition with $\Delta J = 2$, which are greatly affected by the coordination environment. While Eu^{3+} $^5D_0 \rightarrow {}^7F_1$ transition is magnetic dipole transition with much less sensitivity to the coordination environment. Therefore, ratio values of RO can determine the local surrounding of Eu^{3+} (Zhang and Wang 1999). As shown in figure 3C, it is found that the RO values decrease with increasing of PO_4^{3-} content. This can be ascribed to the variation in the degree of covalence of the Eu^{3+}–O^{2-} band. The RO ratio is related to many factors, including the site symmetry, charge-to-radius of Ln^{3+} and electronegativity of the next-neighbour element (Blasse and Grabmeter 1994). P atom possesses higher electronegativity than V atom and the substitution of P by V has influence on the property of ion bond in $P_xV_{1-x}O_4^{3-}$ host, which further affects the energy excitation of $P_xV_{1-x}O_4^{3-}$ group. Subsequently, different compositions of^{-} host matrices will have some influence on the luminescence of phosphor $Sr_3Y(P_xV_{1-x}O_4)_3$ doped with Eu^{3+}. Because the Z/R value of P is higher than that of V, the substitution of P by V can increase the covalent interaction of O^{2-}–Eu^{3+} and the RO intensity ratio of Eu^{3+}. In addition, compared to the pure $Sr_3Y(P_xV_{1-x}O_4)_3$: Eu^{3+} without vanadium substitution, the photoluminescent intensities of Eu^{3+} are improved (Xiao *et al* 2007), which suggests that the introduction of vanadium are favourable for the luminescence of Eu^{3+} because VO_4^{5-} group is a suitable host or sensitizer for Eu^{3+}.

From the above result, we choose the $Sr_3Y(P_{0.3}V_{0.7}O_4)_3$ as the host lattice to examine the optimum concentration of Eu^{3+}. From figure 4, it is also observed that the intensity increases with the increase in concentration at the range of 1–5 mol % for doping concentration, and when the concentration reaches 7 mol %, the corresponding intensity dramatically decreases. This is the typical property for rare earth ions named as concentration quenching, caused by many factors such as interaction between rare earth ions themselves. The Ln–Ln distance becomes considerably shorter when the Ln concentration is higher. This, in turn, could markedly increase the attractions between the lanthanide ions. Energy transfer between the lanthanide ions themselves is a nonradiative process, which partially contributes to the quenching of the Ln^{3+} ions.

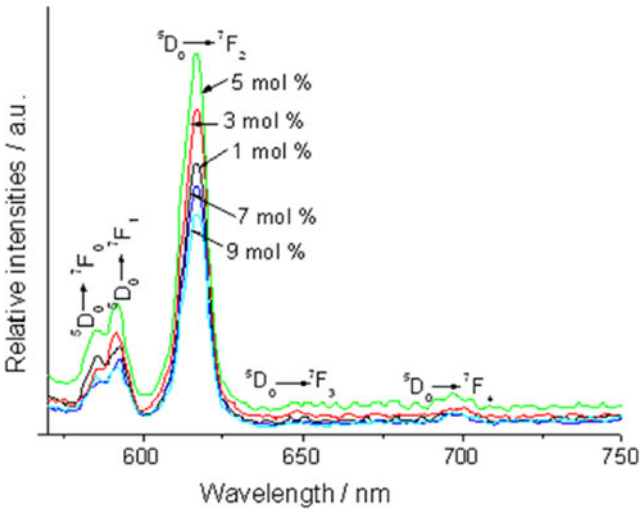

Figure 4. Emission spectra of $Sr_3Y(P_{0.3}V_{0.7}O_4)_3$: x mol %Eu^{3+} ($x = 1, 3, 5, 7, 9$).

4. Conclusions

In summary, we have synthesized the $Sr_3Y(P_xV_{1-x}O_4)_3$: Eu^{3+} with different content ratio of P to V from the hybrid precursors. From the XRD and SEM, it is found that these products belong to the large family of the eulytite type compounds and present column-like submicrocrystalline with 0·25–1 μm in dimensions. Besides, $Sr_3Y(P_{0.3}V_{0.7}O_4)_3$: Eu^{3+} exhibits the strongest luminescence among these phosphors and RO values of Eu^{3+} strongly depends on the content ratio of P to V, suggesting that the RO value increases with the increase of V content due to the different electronegativities of V and P. It is also found that the peak position of charge transfer band (CTB) for O^{2-}–Eu^{3+} in $Sr_3Y(P_xV_{1-x}O_4)_3$ shifts to longer wavelength with the increase of the V content. Furthermore, the luminescence of $Sr_3Y(P_{0.3}V_{0.7}O_4)_3$: Eu^{3+} shows that the optimum concentration of Eu^{3+} is 5 mol % and the concentration quenching took place because of the increased attractions between the lanthanide ions when the Eu^{3+} concentration is higher.

Acknowledgement

The work is supported by the Developing Science Fund, Tongji University, for Excellent Youth Scientists.

References

Alifanti M, Baps B, Blangenois N, Naud J, Grange P and Delmon B 2003 *Chem. Mater.* **15** 395

Blasse G and Grabmeter B C 1994 *Luminescent materials* (Berlin: Springer Verlag)

Burland D M, Miller R D and Walsh C A 1994 *Chem. Rev.* **94** 31

Chuai X H, Zhang H J and Li F S 2000 *Mater. Lett.* **46** 244

Dhanaraj J, Jagannathan R, Kutty T R N and Lu C H 2001 *J. Phys. Chem.* **B105** 11098
Hoogendop M F, Schipper W J and Blasse G 1994 *J. Alloys Compds.* **205** 249
Huang H H and Yan B 2004 *Solid State Commun.* **132** 773
Huang H H and Yan B 2007 *Opt. Mater.* **29** 1706
Huignard A, Buissette V, Franville A C, Gacoin T and Boilot J P 2003 *J. Phys. Chem.* **B107** 6754
Kaminskii A A, *et al* 1976 *Phys. Status Solidi* **A33** 737
Kang C C, Liu R S, Chang J C and Lee B J 2003 *Chem. Mater.* **15** 3966
Liang H B, Tao Y, Xu J H, He H, Wu H, Chen W X, Wang S B and Su Q 2004 *J. Solid State Chem.* **177** 901
Nair B S K, Sundar D, Tomita A, Hoffmann W and Lakshmanan A R 2000 *J. Lumin.* **86** 67
Okamoto S and Yamamoto H 2001 *Appl. Phys. Lett.* **78** 655
Pizani P S, *et al* 2000 *Appl. Phys. Lett.* **77** 824
Rogemond F, Pedrini C, Moine B and Boulon G 1985 *J. Lumin.* **33** 455
Rullens F, Laschewsky A and Devillers M 2006 *Chem. Mater.* **18** 771
Stouwdam J W and Van Veggel F C J M 2002 *Nano Lett.* **27** 733
Su Q, Zhang H J, Pei Z W and Zou F 1989 *Rare earths spectroscopy*. in *Proc. 2nd int. symp. RES* (ed.) O Su (Singapore: World Scientific) pp 214
Szuszkiewicz W and Znamierowska T 1990 *J. Solid State Chem.* **88** 406
Xiao X Z and Yan B 2006 *Appl. Phys.* **A88** 333
Xiao X Z, Xu S and Yan B 2007 *J. Alloys Compds.* **429** 255
Yan B and Xiao X Z 2006 *Opt. Mater.* **28–29** 498
Yan B, Su X Q and Zhou K 2006 *Mater. Res. Bull.* **41** 134
Yu M, Lin J, Wang Z, Fu J, Wang S, Zhang H J and Han Y C 2002 *Chem. Mater.* **14** 2224
Zhou L and Yan B 2006 *Ceram. Int.* **32** 207
Zhang Y and Wang M Q 1999 *Mater. Lett.* **41** 149